The evolution histories of five clusters of galaxies

Florence Durret [1,2] and Gastão B. Lima Neto[3]

1. IAP, CNRS UMR 7095 , Université Pierre et Marie Curie, 98bis Bd Arago, 75014 Paris, France
2. Observatoire de Paris, LERMA, UMR 8112, 61 Avenue de l'Observatoire, 75014 Paris, France
3. Instituto de Astronomia, Geofisica e C. Atmosf./USP, R. do Matão 1226, 05508-090 São Paulo, Brazil

Summary

XMM-Newton and Chandra have extensively shown that clusters of galaxies are not often as relaxed as previously believed.
With its high sensitivity, XMM-Newton allows to obtain temperature, metallicity, pressure and entropy maps which give detailed informations on the cluster properties and evolutionary scenarios.
We present here results for five medium-redshift clusters (z=0.223-0.313) ranging from almost relaxed to strongly perturbed by ongoing merging processes.

The data and data reduction

The data were all taken from the XMM-Newton archive and are presented in Table 1.

Table 1. Summary of the XMM-*Newton* data.

Cluster	Obs. nb	Initial exp. time (s) MOS1/MOS2/PN	Clean exp. time (s) MOS1/MOS2/PN	redshift	scale (1 arcmin) (h_{70}^{-1} kpc)	Galactic N_H (10^{20} cm^{-2})
Cl 2137.3-2353	0008830101	21833/21834/17567	9714/ 9716/ 6039	0.313	275.1	3.55
Abell 2390	0111270101	22223/22227/17985	9381/ 8861/ 6337	0.230	220.5	6.80
Abell 68	0084230201	29243/29259/22295	23750/22365/15573	0.255	238.0	4.94
Abell 1763	0084230901	25881/25898/19451	11996/12335/ 8444	0.223	215.3	5.87
Abell 2744	0042340101	17390/17420/11581	13673/13627/ 9174	0.306	272.2	1.31

The ODFs were treated following the standard procedure:
The background was taken from blank sky templates by Lumb et al. (2002), with a careful analysis of possible soft excess or unusual absoption.
Maps were computed by combining MOS1, MOS2 and pn data following an adaptive pixel procedure described in Durret et al.(2005) and Lima Neto & Durret (2007).
The event files are rebinned with a pixel size of 12.8x12.8 arcsec^2. For each pixel the RMF and ARF are computed and a MEKAL plasma model is fit using XSPEC v11.2.
The maps were computed with an adaptive kernel technique, adjusting spatially the minimum net count number before the spectral fit.
A minimum number of 900 counts is set in each pixel after background subtraction.

MEKAL one-component fits (left) and VMEKAL fits (right). Error bars are 90% confidence level)

Table 2. X-ray gas: MEKAL one component fits. Error bars are 90% confidence level.

	Cl 2137	Abell 2390	Abell 68	Abell 1763	Abell 2744
R (arcmin/kpc)	2.0/550	3.5/772	3.5/833	3.5/754	1.7/454
kT (keV)	4.56 ± 0.16	9.46 ± 0.32	8.99 ± 0.37	5.38 ± 0.18	9.49 ± 0.51
$Z(Z_\odot)$	0.38 ± 0.06	0.31 ± 0.05	0.23 ± 0.06	0.24 ± 0.04	0.21 ± 0.07
N_H(10^{20} cm^{-2})*	3.55	6.80	4.94	5.87	1.31
χ^2/dof	892/893	1805/1596	1835/1468	1593/1239	1046/1027
kT (keV)	4.54 ± 0.19	7.98 ± 0.30	6.82 ± 0.30	7.38 ± 0.30	9.40 ± 0.67
$Z(Z_\odot)$	0.37 ± 0.06	0.29 ± 0.04	0.22 ± 0.04	0.27 ± 0.05	0.20 ± 0.07
N_H (10^{20} cm^{-2})	3.69 ± 0.44	8.82 ± 0.32	8.27 ± 0.40	< 0.3	1.40 ± 0.40
χ^2/dof	891/892	1685/1595	1627/1467	1295/1238	1046/1026
f_X[0.5-2 keV]	2.2 ± 0.1	7.0 ± 0.2	5.2 ± 0.1	3.4 ± 0.2	1.8 ± 0.1
f_X[2.0-10.0 keV]	2.4 ± 0.1	12.8 ± 0.5	5.5 ± 0.1	4.7 ± 0.3	3.1 ± 0.2
L_X[0.5-2.0 keV]	6.2 ± 0.3	9.8 ± 0.5	3.8 ± 0.1	4.6 ± 0.4	4.1 ± 0.4
L_X[2.0-10.0 keV]	8.8 ± 0.5	20.2 ± 1.0	7.2 ± 0.2	7.4 ± 0.7	9.2 ± 0.9
L_{bolom}	20.0 ± 1.0	42.7 ± 2.0	15.2 ± 0.4	16.0 ± 1.5	19.8 ± 2.0

The * subscript indicates fixed values.
Unabsorbed fluxes are in units of 10^{-12} erg s^{-1} cm^{-2}; luminosities are in units of $10^{44} h_{70}^{-2}$ erg s^{-1}.

Table 3. X-ray gas: VMEKAL fits

	Cl 2137	Abell 2390	Abell 68	Abell 1763	Abell 2744
kT (keV)	4.57 ± 0.12	8.07 ± 0.20	6.94 ± 0.20	5.13 ± 0.16	9.70 ± 0.44
N_H (10^{20} cm^{-2})	3.69 ± 0.33	8.80 ± 0.25	8.08 ± 0.32	5.87^*	1.14 ± 0.27
χ^2/dof	890/898	1671/1601	1606/1473	1807/1308	1038/1021
Fe	0.31 ± 0.03	0.23 ± 0.02	0.17 ± 0.02	0.25 ± 0.04	0.17 ± 0.04
Ne				1.25 ± 0.58	1.25 ± 0.57
Mg	0.64 ± 0.34	0.85 ± 0.34	1.10 ± 0.37		0.77 ± 0.68
Si	0.34 ± 0.16	0.48 ± 0.18	0.20 ± 0.18		0.77 ± 0.37
O	0.38 ± 0.18	0.32 ± 0.20		4.14 ± 0.63	
Ni	0.60 ± 0.54	1.27 ± 0.41	1.54 ± 0.47	2.36 ± 1.05	
S			0.31 ± 0.22		

Discussion

- **Cl 2137.3-23** is quite relaxed but shows a hotter region to the northwest and a higher metallicity strip along a region extending southeast to northwest. This suggests a past merger which has crossed the cluster from the southeast several Gyr ago. It shows Mg and Ni overabundances.
- **Abell 68** is also hot and X-ray luminous and its maps also suggest the existence of previous mergers several Gyr ago.
- **Abell 2390** is hot and massive with some evidence for previous mergers in the north-south direction.
- **Abell 1763** has a long emission tail to the southwest, cooler than the main cluster (3.4 keV instead of almost 10 keV for the main cluster). Its temperature and metallicity maps are highly perturbed . As confirmed by a double bent radio source, there is a merging going on from the southwest to the north east. Besides, the higher temperature to the northwest of the centre suggest that a second more recent merger has taken place from the southeast towards the northwest.
- **Abell 2744** is a cluster undergoing several major mergers, both coming from the southeast (also see Zhang et al. 2004 and Finoguenov et al. 2005). A second more recent minor merger is also probably coming from the northwest.

A detailed description of this work can be found in Lima Neto & Durret (2007, A&A submitted)

References

Durret F., Lima Neto G.B., Forman W. 2005, A&A 432, 809
Finoguenov A., Böhringer H., Zhang Y.-Y. 2005, A&A 442, 827
Lima Neto G.B & Durret F. 2007, A&A submitted
Lumb D.H., Warwick R.S., Page M., De Luca A. 2002, A&A 389, 93
Zhang Y.-Y., Finoguenov A., Böhringer H. et al. 2004, A&A 413, 49

The more or less relaxed clusters Cl 2137.3-2353 (z=0.313), Abell 68 (z=0.255) and Abell 2390 (z=0.230)

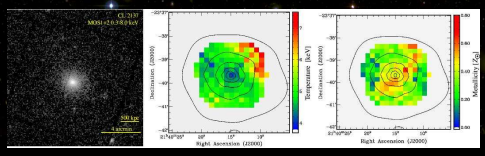

Fig. 1. Cl 2137.3-2353. Left: emission map. Middle: temperature map. Right: metallicity map.

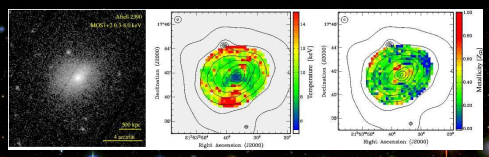

Fig. 2. Same as Fig.1 for Abell 68.

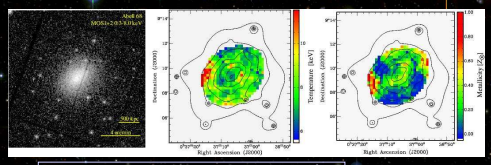

Fig. 3. Same as Fig. 1 for Abell 2390.

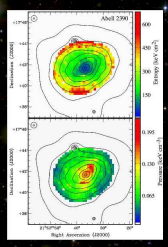

Fig.4. Pressure and entropy maps for Abell 2390.

The perturbed clusters Abell 1763 (z=0.223) and Abell 2744 (z=0.306)

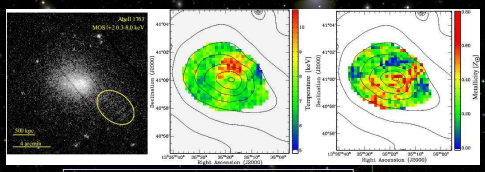

Fig. 5. Same as Fig.1 for Abell 1763.

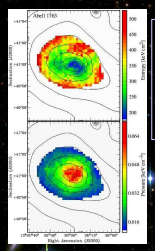

Fig. 6. Pressure and entropy map for Abell 1763.

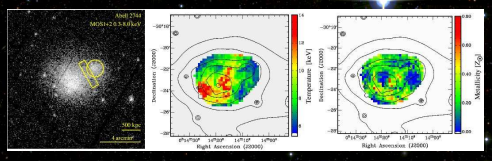

Fig. 7. Same as Fig.1 for Abell 2744.

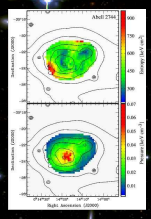

Fig. 8. Pressure and entropy map for Abell 2744.

Quality of the maps: two tests on Abell 1763

Fig. 9.
Top: relative error on the temperature σ_{kT}/kT.
Middle: relative error on the metallicity σ_Z/Z.
Bottom: reduced χ^2 map.

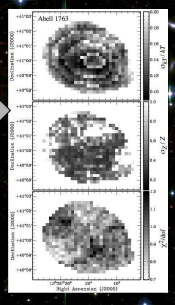

Fig. 10.
Comparison between the temperature maps of Abell 1763.
Top: NH fixed to the Galactic value.
Bottom: NH left as a free parameter.

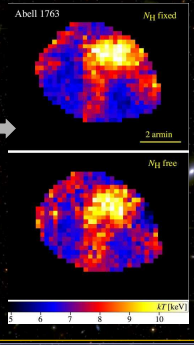

Acknowledgements. We acknowledge financial support from the CAPES/COFECUB. F.D. acknowledges support from CNES and PNC, CNRS/INSU, and G.B.L.N. acknowledges support from the CNPq and FAPESP.